LA-13147

General-Purpose Heat Source: Research and Development Program

Radioisotope Thermoelectric Generator Impact Tests: RTG-1 and RTG-2

Los Alamos
NATIONAL LABORATORY

Los Alamos National Laboratory is operated by the University of California for the United States Department of Energy under contract W-7405-ENG-36.

Edited by Candia Barraclough, Infomatrix, for Group CIC-1.

This work was supported by the U.S. Department of Energy, Office of Nuclear Energy, Office of Special Applications.

An Affirmative Action/Equal Opportunity Employer

DISCLAIMER

LA-13147

UC-500
Issued: July 1996

General-Purpose Heat Source: Research and Development Program

Radioisotope Thermoelectric Generator Impact Tests: RTG-1 and RTG-2

M. A. H. Reimus
J. E. Hinckley
T. G. George

Los Alamos
NATIONAL LABORATORY
Los Alamos, New Mexico 87545

GENERAL-PURPOSE HEAT SOURCE: RESEARCH AND DEVELOPMENT PROGRAM

RADIOISOTOPE THERMOELECTRIC GENERATOR IMPACT TESTS: RTG-1 AND RTG-2

by

M. A. H. Reimus, J. E. Hinckley, and T. G. George

ABSTRACT

The General-Purpose Heat Source (GPHS) provides power for space missions by transmitting the heat of ^{238}Pu decay to an array of thermoelectric elements in a radioisotope thermoelectric generator (RTG). Because the potential for a launch abort or return from orbit exists for any space mission, the heat source response to credible accident scenarios is being evaluated. The first two RTG Impact Tests were designed to provide information on the response of a fully loaded RTG to end-on impact against a concrete target. The results of these tests indicated that at impact velocities up to 57 m/s the converter shell and internal components protect the GPHS capsules from excessive deformation. At higher velocities, some of the internal components of the RTG interact with the GPHS capsules to cause excessive localized deformation and failure.

I. INTRODUCTION

The General-Purpose Heat Source (GPHS) is a modular component of the radioisotope thermoelectric generators (RTGs) that will provide power for the National Aeronautics and Space Administration's (NASA's) Cassini mission to Saturn. An RTG generates electric power by using the heat of ^{238}Pu α-decay to create a temperature differential across a thermoelectric array. Each RTG is loaded with 18 GPHS modules, and each GPHS module (Figure 1) contains four $^{238}PuO_2$ fuel pellets that provide a total thermal output of 250 W. Each fuel pellet is encapsulated in a vented, DOP-26 iridium alloy shell. Two capsules are held in a Fineweave-Pierced Fabric* (FWPF) graphite impact shell (GIS), and two GISs are contained within an FWPF aeroshell.

*Fineweave-Pierced Fabric 3-D carbon/carbon composite, a product of AVCO Systems Division, 201 Lowell St., Wilmington, MA 01887.

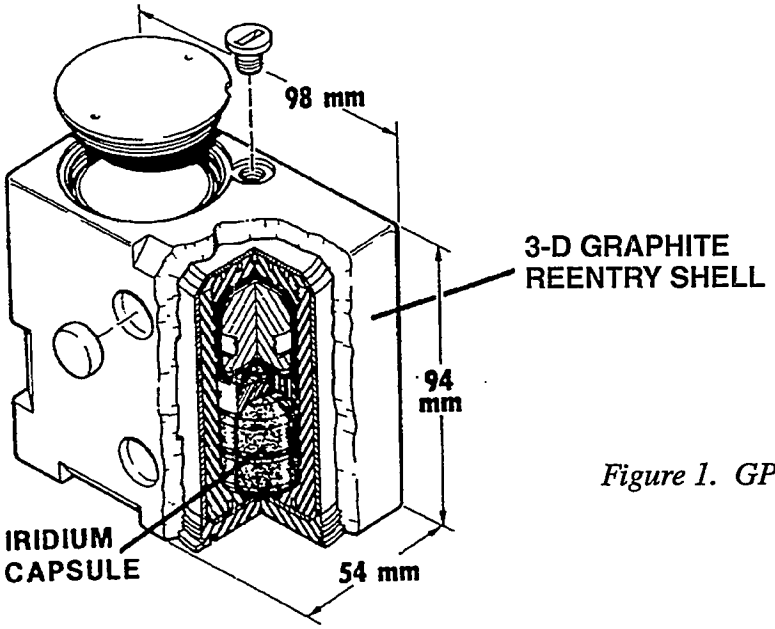

Figure 1. GPHS Module.

Because the potential for a launch abort or return from orbit exists for any space mission, the GPHS response to credible accident scenarios is being evaluated.[1] Previous testing conducted in support of the Galileo and Ulysses missions documented the response of the GPHS heat source to a variety of fragment-impact, aging, atmospheric reentry, and Earth impact conditions[2-9]. Tests that required field testing of heat source and RTG components (such as solid-propellent fire, explosive overpressure, large fragment interaction, etc.) were performed using GPHS capsules fueled with $^{238}UO_2$ (^{235}U-depleted)[10-14].

The end-on RTG impact tests were designed to evaluate the response of GPHSs, GPHS modules and loaded radioisotope thermoelectric generators (RTGs) to conditions that may be experienced as a result of potential on- and near-pad accidents involving failures of the Cassini spacecraft and/or launch vehicle. Specifically, these impact tests were designed to provide information on the response of a loaded RTG to end-on impact against concrete typical of installations at Kennedy Space Center. These tests also utilized GPHS capsules fueled with $^{238}UO_2$.

II. BACKGROUND

A. Fabrication of Urania Pellets

The urania pellets used in this study were fabricated from urania powder produced by Oak Ridge National Laboratory (urania lot # NF-30-4225). All of the pellets used were fabricated by cold pressing followed by sintering. The fabrication technique is described in detail in the following sections.

The urania powder was mixed with a solution of cetyl alcohol (binder) dissolved in acetone. The amount of cetyl alcohol used was approximately two percent of the weight of urania powder. The amount of acetone used was 0.25 ml per gram of urania. The urania/alcohol mixture was gently heated with a heat lamp and blended until dry. This material was then passed through a 30-mesh sieve to break up any agglomerates. The material was then isostatically pressed at 25 to 30 ksi, then crushed and passed through a 60-mesh sieve (250 μm).

After sieving, approximately 150 g of the treated urania was loaded into a graphite die and then pressed in a Carver 25 ton press for one minute at 20 tons of load. The rough pellet was then removed and sintered at 1825°C for four hours in humidified H_2 (45°F dewpoint). The pellet was ground to final dimensions and then vacuum outgassed at 250°C for two hours.

B. Source and History of Test Components

The graphite components used in the test series were obtained from EG&G Mound Applied Technologies (EG&G MAT). Each of the converter sections was loaded with a stack made up of eight FWPF graphite modules and one POCO (polycrystalline graphite) module that was 0.24 in. less than full module height. This POCO module, designated number 9, was located at the end of the stack opposite the RTG dome (the impacted end) and contained a molybdenum disc with mass equivalent to that of four simulant-fueled GPHSs. In the first end-on RTG impact test (RTG-1), the first three modules (number 1 is at the impact end) were fabricated from FWPF graphite and contained FWPF graphite GISs loaded with urania-fueled GPHSs with flight-quality iridium cladding. Modules 4 and 5 were fabricated of FWPF graphite and contained POCO grade AXF 5Q GISs loaded with urania-fueled GPHSs with engineering quality iridium cladding. Modules 6, 7, and 8 consisted of FWPF graphite modules containing POCO grade AXF 5Q GISs loaded with molybdenum slugs fabricated with GPHS exterior dimensions. In the second end-on RTG impact test (RTG-2), the first four modules were fabricated from FWPF graphite and contained FWPF GISs loaded with urania-fueled GPHSs with flight-quality iridium. Modules 5 and 6 were fabricated of FWPF and contained POCO AXF 5Q GISs loaded with urania-fueled GPHSs with engineering quality iridium. Modules 7 and 8 are similar to 5 and 6 with the exception of being loaded with molybdenum slugs. Components of the GPHS module stacks for RTG-1 and RTG-2 are identified in Tables I and II.

TABLE I. RTG-1 Test Components

Stack Location	#1	#2	#3	#4	#5	#6	#7	#8
Module ID	007	009	1011	1013	1015	1018	018	016
A GIS Assembly								
GIS	2001[a]	2003[a]	2005[a]	92001[b]	92003[b]	92005[b]	92007[b]	92009[b]
Floating Membrane	4001	4003	4005	4007	4009	4011	4145	4147
GPHS, Open End	SC0077	SC0081	SC0085	SC0065	SC0069	6AO	7AO	8AO
GPHS, Blind End	SC0076	SC0080	SC0084	SC0064	SC0068	6AB	7AB	8AB
C GIS Assembly								
GIS	2002[a]	2004[a]	2006[a]	92002[b]	92004[b]	92006[b]	92008[b]	92010[b]
Floating Membrane	4002	4004	4006	4008	4010	4012	4146	4148
GPHS, Open End	SC0079	SC0083	SC0088	SC0067	SC0071	6CO	7CO	8CO
GPHS, Blind End	SC0078	SC0082	SC0087	SC0066	SC0070	6CB	7CB	8CB

[a] Fine Weave-Pierced Fabric (FWPF) graphite.
[b] POCO graphite.

TABLE II. RTG-2 Test Components

Stack Location	#1	#2	#3	#4	#5	#6	#7	#8
Module ID	1001	1014	019	020	8003	8004	8005	8007
A GIS Assembly								
GIS Insulating Sleeve	NR[a]	NR[a]	NR[a]	NR[a]	B47-5	B47-6	B47-9	B49-4
GIS	2009[b]	2011[b]	2014[b]	2013[b]	92013[c]	92015[c]	92017[c]	92011[c]
Floating Membrane	4013	4060	4150	4152	4145	4147	104001	104003
GPHS, Open End	SC0090	SC0094	SC0103	SC0108	SC0069	SC0101	7AO	8AO
GPHS, Blind End	SC0089	SC0093	SC0097	SC0106	SC0068	SC0100	7AB	8AB
C GIS Assembly								
GIS Insulating Sleeve	NR[a]	NR[a]	NR[a]	NR[a]	B47-8	B47-7	B48-3	B49-5
GIS	2010[b]	2012[b]	2015[b]	2016[b]	92014[c]	92016[c]	92018[c]	92012[c]
Floating Membrane	4014	4149	4151	4153	4146	4148	104002	1040004
GPHS, Open End	SC0092	SC0096	SC0105	SC0107	SC0071	SC0109	7CO	8CO
GPHS, Blind End	SC0091	SC0095	SC014	SC0086	SC0070	SC0102	7CB	8CB

[a] Not recorded - insulating sleeve installed at Mound.
[b] Fine Weave-Pierced Fabric (FWPF) graphite.
[c] POCO graphite.

The modules consisted of FWPF aeroshells containing two GISs designated as A and C. The A GIS is inserted in the A GIS cavity. This cavity is identified by a small dimple on the face of the aeroshell that has flight control bevels machined on the edges. The dimple is located on the corner of the face closest to the A GIS cavity end cap.

The concrete target for each test was 36 in. × 48 in. × 18 in. thick. The concrete was provided by the US Air Force at Cape Canaveral. It is typical of the concrete used for launch pads and other installations in the area. Each concrete slab was oriented with the 36 in. edge horizontal and the 48 in. edge vertical. This face was centered across the sled track.

The RTG converter shells used in these tests were provided by Lockheed Martin. Each one consisted of approximately one half of a converter housing. The outboard end of the converter, which was impacted against the concrete, included the heat source support system (including end foil insulation) and the pressure dome. The following Lockheed Martin drawings define the test articles tested: converter assembly, 23009111; converter shell assembly, 23008093; and heat source assembly, 23009090.

III. EXPERIMENTAL PROCEDURES

A. Pretest Data

The dimensions and weights of the urania pellets were measured and recorded prior to encapsulation. The clads were then submitted for ultrasonic testing (UT) of the girth weld. Table III lists the weights of the urania pellets used in this study. Also listed are the clad vent sets and the UT results.

TABLE III. GPHS Capsules Used in RTG-1 and RTG-2

GPHS ID	PICS#	Max UT Indication, Equil mil	Indication Location, deg	UT Disposition[a]	Pellet ID	Pellet Weight, g
SC0064	9808-30-1812	5.41	129	Reject	1	140.74
SC0065	9808-30-1810	3.96	90	Accept	2	142.39
SC0066	9808-30-1813	6.63	214	Reject	3	142.40
SC0067	9808-30-1814	7.07	316	Reject	4	142.83
SC0068	9808-30-1815	4.93	159	Accept	5	142.30
SC0069	9808-30-1817	4.85	86	Accept	6	141.59
SC0070	9808-30-1818	4.15	48	Accept	7	141.04
SC0071	9808-30-1820	5.49	323	Reject	19	141.65
SC0076	9808-01-2169	2.63	125	Accept	15	147.23
SC0077	9808-01-2170	3.21	76	Accept	16	145.49
SC0078	9808-01-2171	4.43	294	Accept	17	147.27
SC0079	9808-01-2172	3.01	256	Accept	18	145.76
SC0080	9808-01-2174	4.19	80	Accept	25	149.80
SC0081	9808-01-2175	4.05	51	Accept	26	149.12
SC0082	9808-01-2176	2.93	65	Accept	28	149.33
SC0083	9808-01-2177	4.29	146	Accept	29	148.17
SC0084	9808-01-2178	2.76	242	Accept	30A	148.39
SC0085	9808-01-2179	3.58	58	Accept	31A	149.55
SC0086	9808-01-2181	5.28	15	Reject	32A	149.74
SC0087	9808-01-2182	3.59	210	Accept	33A	149.52
SC0088	9808-01-2183	3.92	197	Accept	34A	149.40
SC0089	9808-01-2184	4.02	287	Accept	35A	148.22
SC0090	9808-01-2185	4.26	52	Accept	36A	148.59
SC0091	9808-01-2186	3.73	191	Accept	37A	151.68
SC0092	9808-01-2188	2.66	54	Accept	38A	150.99
SC0093	9808-01-2189	2.49	265	Accept	40A	151.93
SC0094	9808-01-2190	4.12	61	Accept	41A	150.82
SC0095	9808-01-2191	4.55	49	Accept	42A	150.02
SC0096	9808-01-2192	3.42	28	Accept	43A	149.72
SC0097	9808-01-2193	3.35	253	Accept	44A	150.28
SC0100	9808-30-1827	7.46	27	Reject	24	147.69
SC0101	9808-30-1822	3.49	253	Accept	32	149.74
SC0102	9808-30-1823	3.59	258	Accept	40	151.93
SC0103	9808-01-2059	3.83	81	Accept	47	148.30
SC0104	9808-01-2060	4.53	293	Accept	48	146.50
SC0105	9808-01-2061	4.14	60	Accept	50	148.50
SC0106	9808-01-2062	4.14	244	Accept	51	149.40
SC0107	9808-01-2065	5.55	280	Reject	52	148.30
SC0108	9808-01-2066	4.08	44	Accept	53	149.00
SC0109	9808-01-2067	6.99	182	Reject	54	147.60

[a] Reject disposition based on UT reflector >5.2 equivalent mils located in girth weld area.

B. Field Testing

The tests were conducted at the Sandia National Laboratory (SNL) Rocket Sled Test Track area, within Area III. The test hardware consisted of the furnace and its support stand, the rocket sled, the aperture plate, and the concrete block. The furnace, designed to heat its contents in an argon atmosphere, had Canthol elements that were conditioned to reach 1200-1250°C. The furnace had a bottom "door" that could be remotely operated so that the graphite stack could be lowered from the furnace into the converter housing. The support stand was a steel structure that supported the furnace and the graphite stack lowering apparatus. The sled was designed to compress as it impacted the aperture plate. The aperture plate was designed to stop the sled while allowing the RTG housing to pass through an opening to the concrete target. The key features on the sled included the support/rotation shafts, the rear latch mechanism, the shaft rotation DC motor and its corresponding counter weight. The shafts supported the RTG housing and rotated the housing from vertical to horizontal orientation. Hinges in the shafts were designed to allow the shafts to travel forward through access slots in the mounting block as the sled impacted the aperture plate (Figures 2 and 3). The rear latch mechanism locked the RTG assembly in the horizontal orientation and held it in place while it was propelled down the sled track. The counter weight balanced the weight across the sled, thereby ensuring a uniform compression of the sled upon impact with the aperture plate. Los Alamos National Laboratory drawings used for test assembly include:

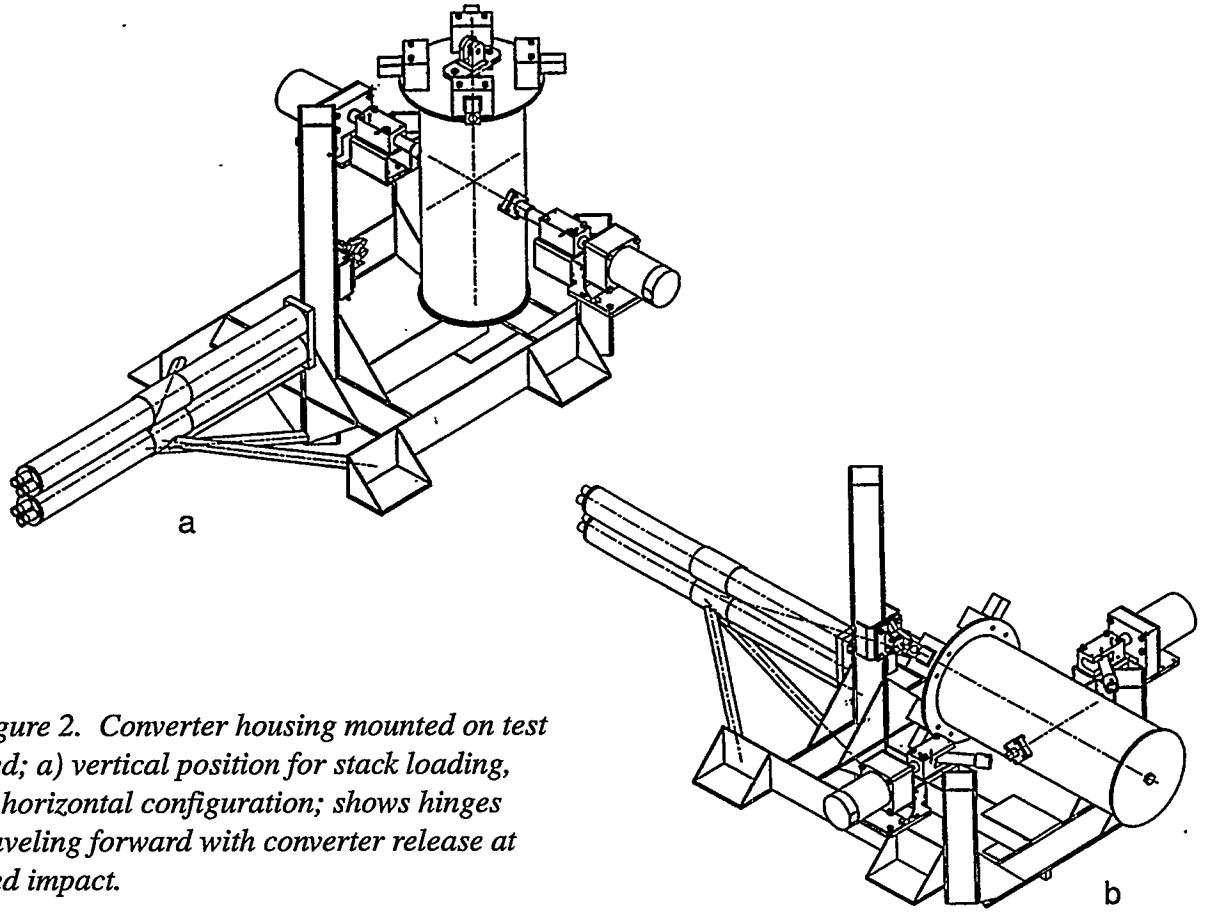

Figure 2. Converter housing mounted on test sled; a) vertical position for stack loading, b) horizontal configuration; shows hinges traveling forward with converter release at sled impact.

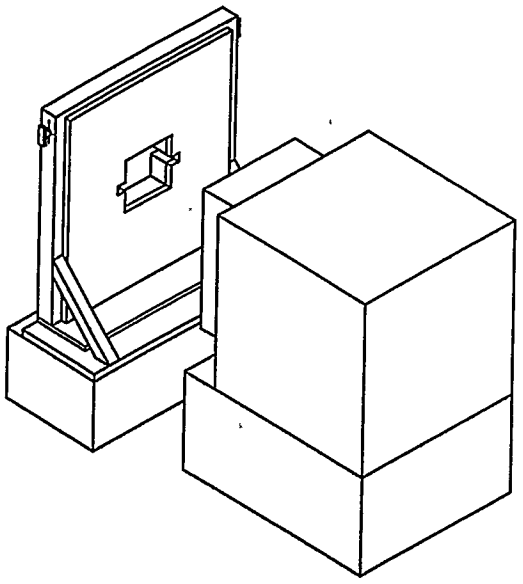

Figure 3. Aperture plate and concrete target.

264-318097101-Safety: RTG Impact Tests, End-on Impact Test Layout
264-318087101 thru 013-Safety: RTG Impact Tests, Furnace Support Stand Assembly
264-318092101 thru 028-Safety: RTG Impact Tests, End-on Impact Tests, Sled Assembly
264-318084101 thru 029-Safety: RTG Impact Tests, Furnace Support Stand Assembly

The graphite module stacks were heated to approximately 1210°C. The rockets were readied and the test sequence began with the remote opening of the furnace door. The stack was then remotely lowered from the furnace into the RTG housing attached to the test sled. The lowering sequence was completed when the latches on top of the housing section engaged, securing the stack within. The RTG was then rotated 90 degrees into the end-on configuration and latched into place with the rear latch mechanism. After the appropriate amount of time had passed for the clads inside the stack to cool to nominally 1093°C (approximately one minute), the rockets on the sled were fired, propelling the sled and its components down the track and into the aperture plate (approximately 1.5 sec). Upon impact with the aperture plate, the sled was stopped and the RTG released through the aperture and impacted the concrete target. The stack cooling characteristics were measured prior to testing at LANL and at the test site at SNL.

IV. RESULTS

A. First End-on Impact Test; RTG-1

One half of a Cassini RTG with a simulant heat source stack made up of FWPF graphite modules loaded with urania-fueled clads and molybdenum slugs was impacted against a 3 ft. × 4 ft. × 18 in. slab of concrete on April 13, 1995. The impact velocity was 57.6 ± 0.3 m/s and the RTG graphite module stack temperature was 1071 ± 5°C. The furnace stand is shown in Figure 4, and the converter mounted on the sled is shown in Figure 5.

The converter rebounded after impact with a modest twisting of the trailing end. The trailing end struck the cushioned rear side of the aperture plate through which the converter traveled

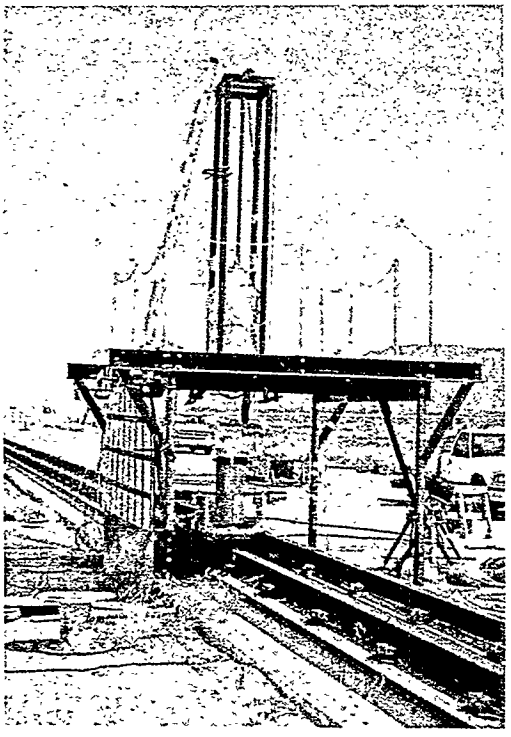

Figure 4. Test stand for Test RTG-1. (Neg B2049, Roll 2, #6)

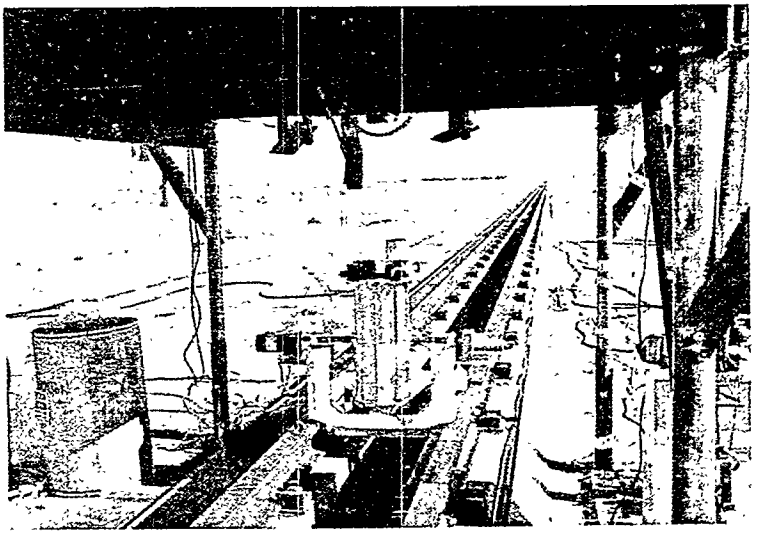

Figure 5. Converter housing mounted on sled for Test RTG-1. (Neg B2049, Roll 1, #8)

upon release from the sled. Most of the failure in the converter housing took place in the upper end of the outboard end above the circumferential rib (Figure 6). This rib was located 2.95 in. from the outboard end flange. There was considerable breakup of the module stack inside the converter. A piece of the stack tie rod and fitting, along with one intact module (Module 9), was ejected from the back end of the converter housing. Intact Modules 8, 7, and 6 fell free from the converter after the test as it was moved to accommodate an argon flush to prevent oxidation of graphite components in the converter (Figure 7).

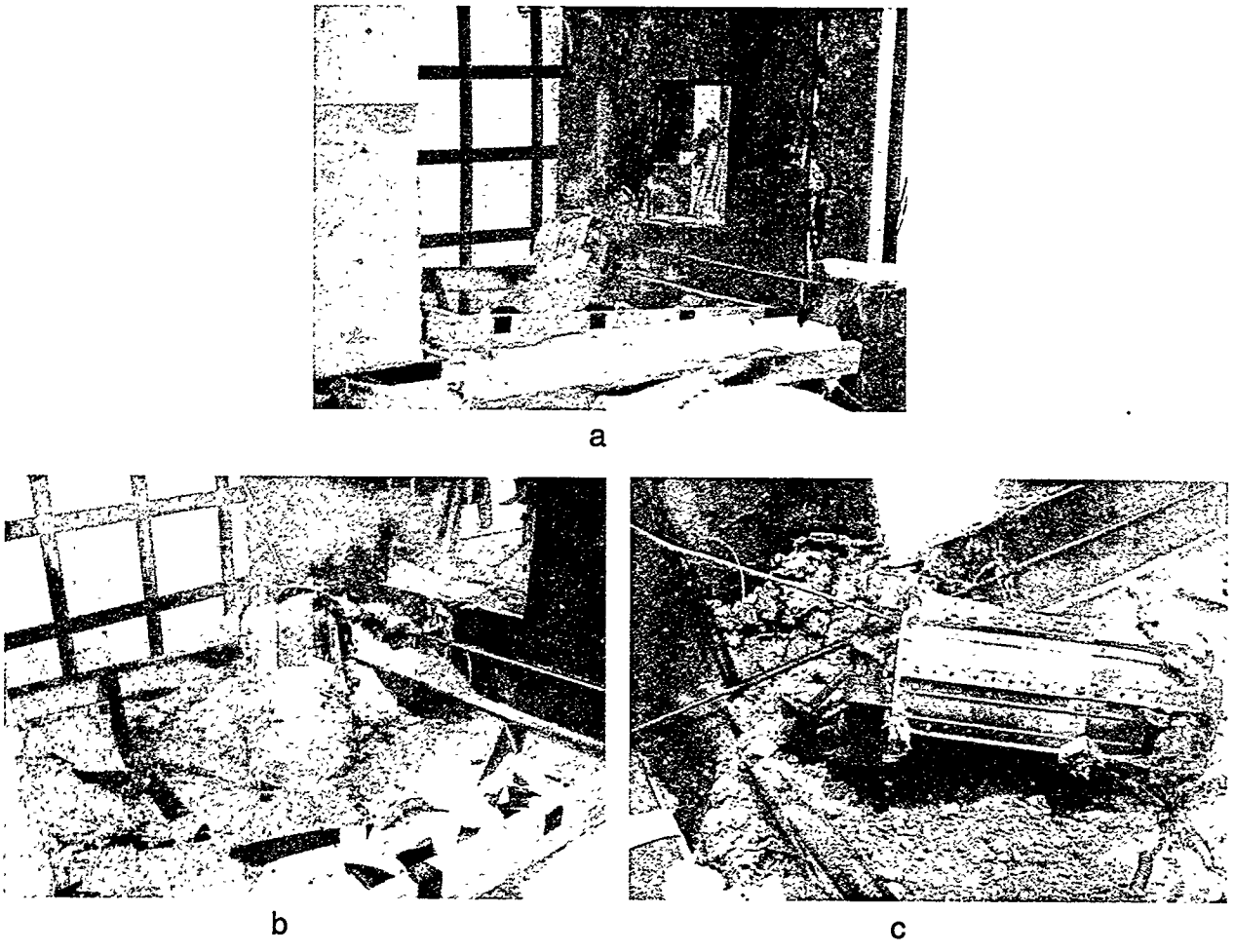

Figure 6. Impacted converter housing, Test RTG-1; (a) side view, (b) close-up of side view, (c) opposite side view, 180 degrees. (NMT-9 Negs B2049, Roll 2, #11; B2049, Roll 2, #32; B2049, Roll 2, #29)

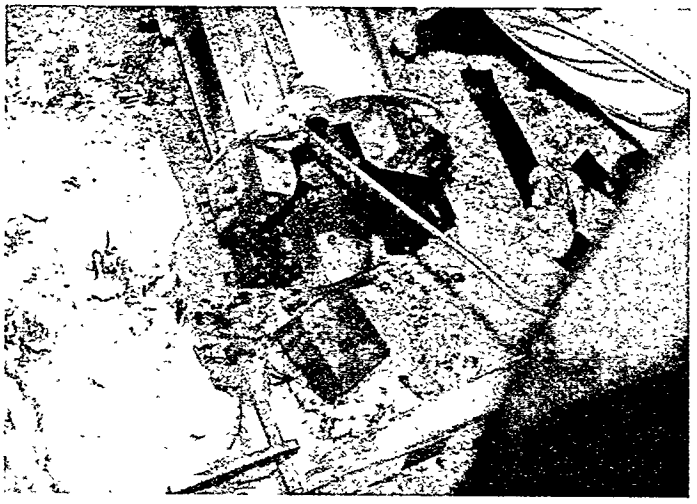

Figure 7. Rear end of impacted converter housing, Test RTG-1. (NMT-9 Neg B2049, Roll 3, #12)

Field observations revealed that one clad had been ejected from its module and GIS but remained in the converter (Figure 8). This clad was observed upon removal of the end four modules. Upon disassembly of the converter in the laboratory, a second clad was observed to have been ejected from its module and GIS. These two clads were determined to have been in the A GIS in Module 2.

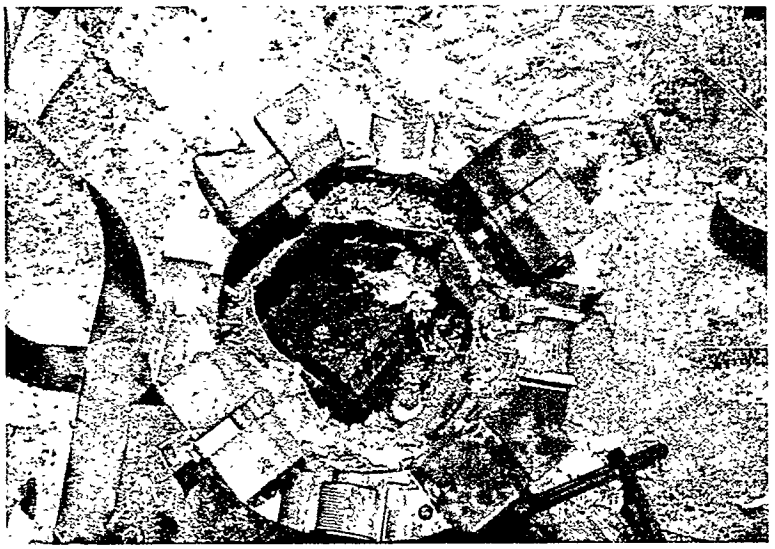

Figure 8. One clad was ejected from its module and remained in the converter, Test RTG-1. (Neg B2049, Roll 3, #24)

Modules 5 and 4 had minor failures. In both modules, two clads were ejected from each module. The GISs that originally contained the clads were shattered. Module 3 split in half, along a line roughly parallel to the GIS cavities. One of the GISs was intact, the other missing a portion of its wall. The clads were completely contained within the two GISs.

The Module 1 and 2 aeroshells were shattered into several pieces. All GISs from these two aeroshells were also shattered into several pieces. One of the arms of the titanium heat source support assembly in the converter housing failed. Two of the heat source support assembly's four stand-offs were also broken (Figure 9). These stand-offs are the probable cause of the higher deformation of the A GISs of Modules 1 and 2.

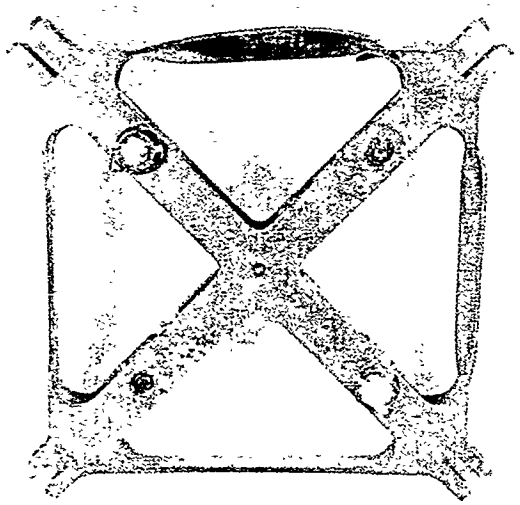

Figure 9. The titanium heat source support assembly recovered from Test RTG-1 converter had failures in one arm and two stand-offs. (NMT-9 Neg 952-91)

Capsule deformations are listed in Table IV. The largest deformations were experienced by the Module 1 clads, as expected. No visible cracks or breeches were observed in any of the clads. Based on historical data, one would expect the strains reported for the capsules in Module 1 to have resulted in breaching cracks.

Clad SC0076 was located in the blind end of the A GIS in Module 1 (Figure 10). This clad had the most deformation, as indicated by strain calculations, of the clads impacted in this test. In spite of its relatively large deformation, neither SC0076 nor any other clad breached. The impact face of this clad was centered at approximately 270 degrees from the weld start. Because this clad was the most highly deformed, it was selected for metallographic examination. It was defueled and the fuel submitted for particle size analysis.

Six sections were cut from SC0076 and submitted for metallographic examination. Examination of the vent revealed typical microstructure. No anomalies were observed in the vent microstructure (Figure 11).

TABLE IV. RTG-1 Capsule Strains

			STRAIN, %[a]			
			Vent Cup, Diametral		Shield Cup, Diametral	
Module	GPHS	Axial	Max.	Min.	Max.	Min.
1	SC0077	8.30	12.60	-15.08	10.71	-4.28
1	SC0076	19.48	20.57	-17.14	15.94	-11.31
1	SC0079	5.84	9.34	-2.06	6.26	-3.77
1	SC0078	5.93	11.65	-8.65	10.37	-5.14
2	SC0081	2.12	6.34	-6.51	4.03	-1.03
2	SC0080	8.72	13.28	-7.80	8.40	-5.91
2	SC0083	4.91	4.88	-3.94	4.88	-3.34
2	SC0082	2.88	6.94	-7.88	4.71	-1.20
3	SC0085	2.29	1.63	-4.37	1.29	-0.51
3	SC0084	1.78	3.34	-3.94	2.49	-1.80
3	SC0088	1.35	1.37	-4.11	0.94	-1.80
3	SC0087	1.02	0.86	-2.40	0.94	-1.63
4	SC0065	1.61	0.51	-1.97	0.77	-1.80
4	SC0064	2.03	1.46	-4.97	1.29	-3.86
4	SC0067	1.02	0.77	-3.00	1.97	-2.40
4	SC0066	2.29	2.14	-3.08	1.89	-3.60
5	SC0069	0.00	-0.26	-0.17	0.26	0.17
5	SC0068	-0.08	-0.34	0.00	0.26	0.26
5	SC0071	-0.85	-0.34	-0.26	0.34	0.17
5	SC0070	-0.08	-0.34	-0.17	0.34	0.17

[a] Engineering strain values based on nominal dimensions (length = 1.181 in. and cup diameter = 1.167 in.)

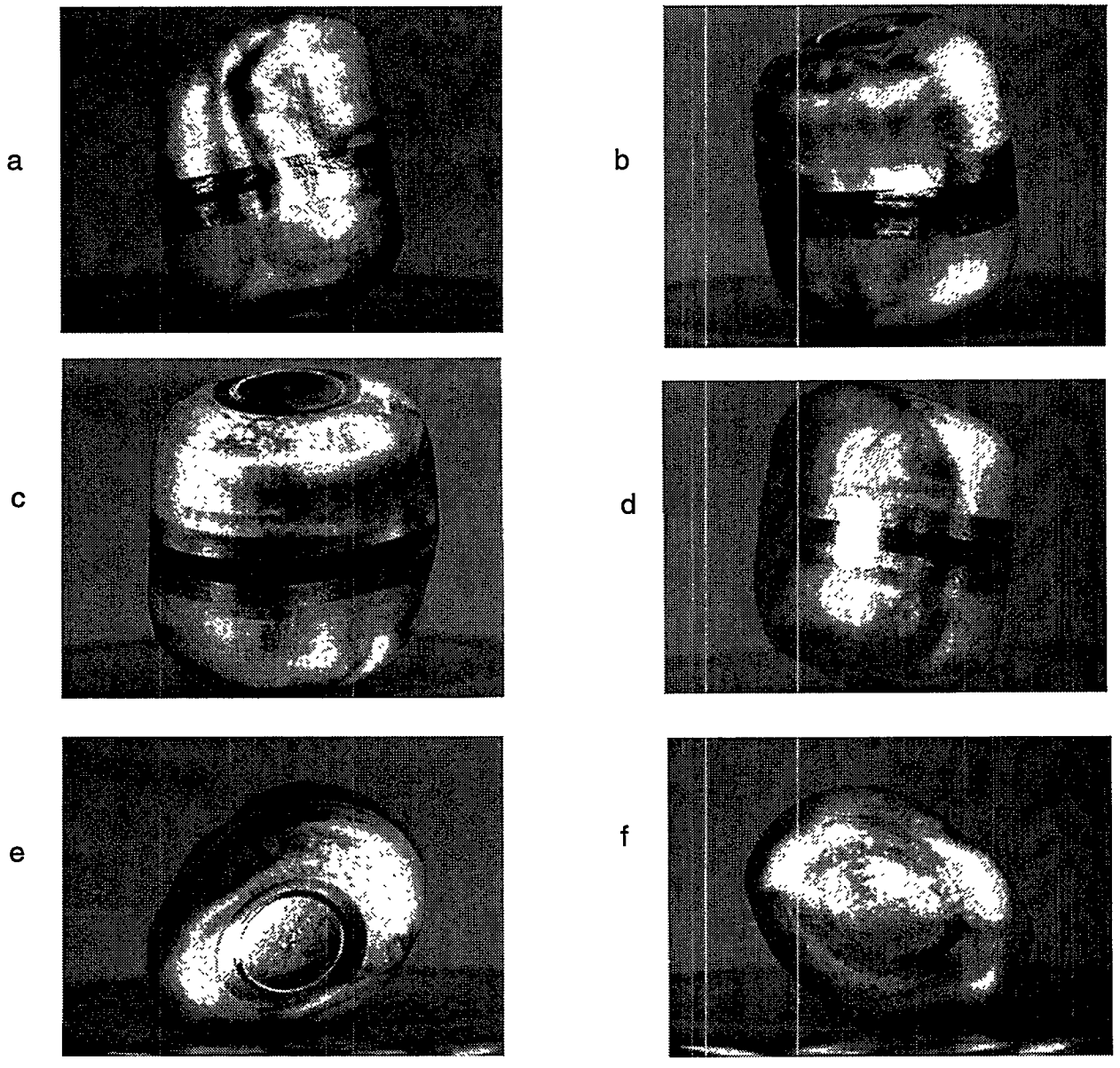

Figure 10. SC0076 experienced the greatest amount of strain in Test RTG-1; (a) impact face, (b) profile, (c) trailing face, (d) opposite profile, (e) vent end, (f) blind end, (g) fuel fragmentation. (NMT-9 Negs 952-17, 952-14, 952-15, 952-16, 952-19, 952-18, 9510-70)

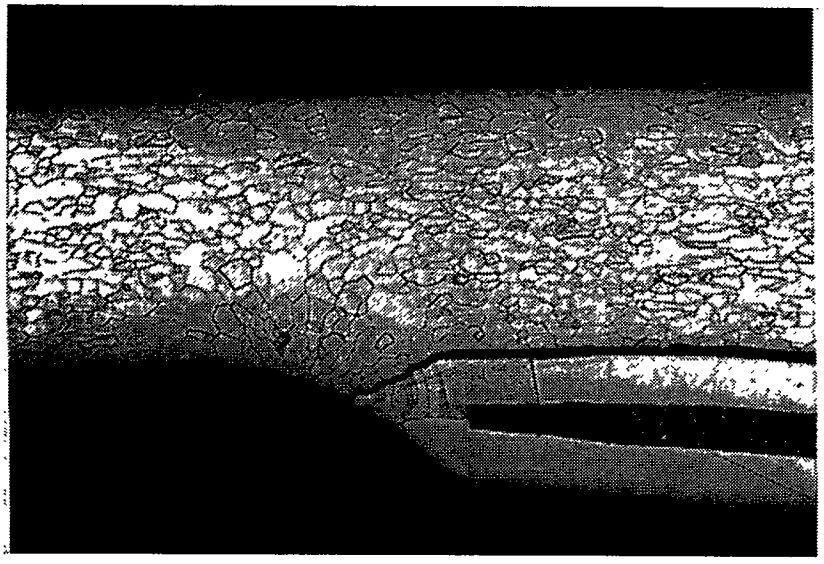

a

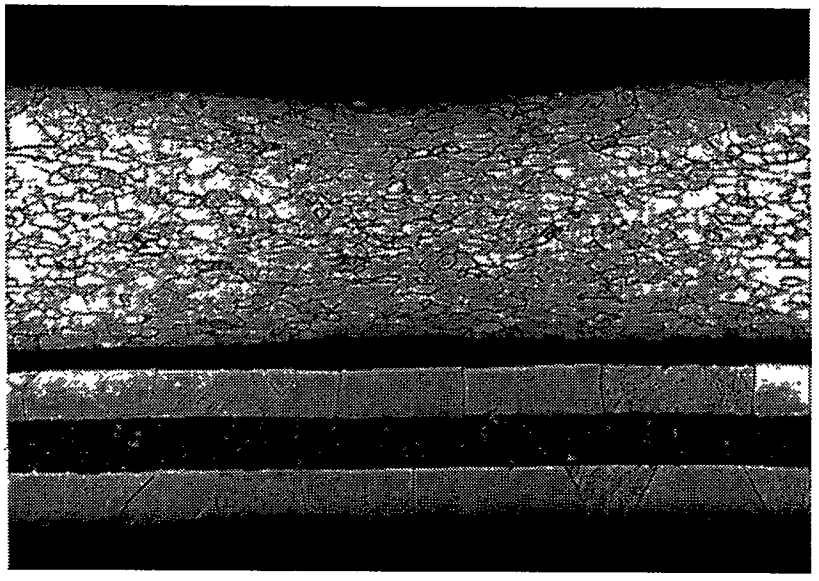

b

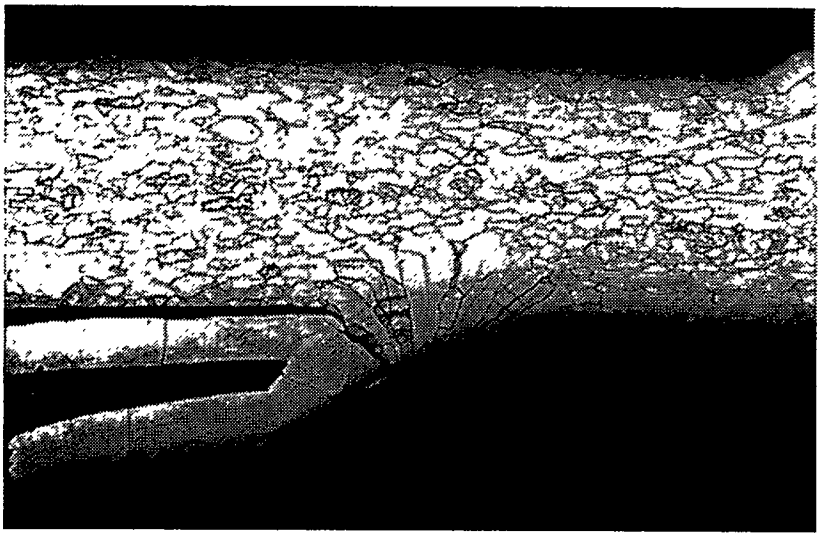

c

Figure 11. The microstructure of capsule SC0076 vent shows no anomalies; etched, 50× magnification; (a) vent edge, (b) center area, (c) opposite edge. (NMT-9 Negs 9511-75, 9511-76, 9511-74)

The microstructures of the single-pass weld and weld overlap areas were typical of the microstructures usually observed in these areas (Figure 12). The grain size in the single-pass weld area averaged 10.7 grains/wall thickness (78.1 μm/grain), and the grain size in the weld overlap area averaged 9.5 grains/wall thickness (84.7 μm/grain). The microstructures of the vent and shield cup walls were also typical. The grain sizes in these areas are given in Table V. The fuel particle size analysis is given in Table VI.

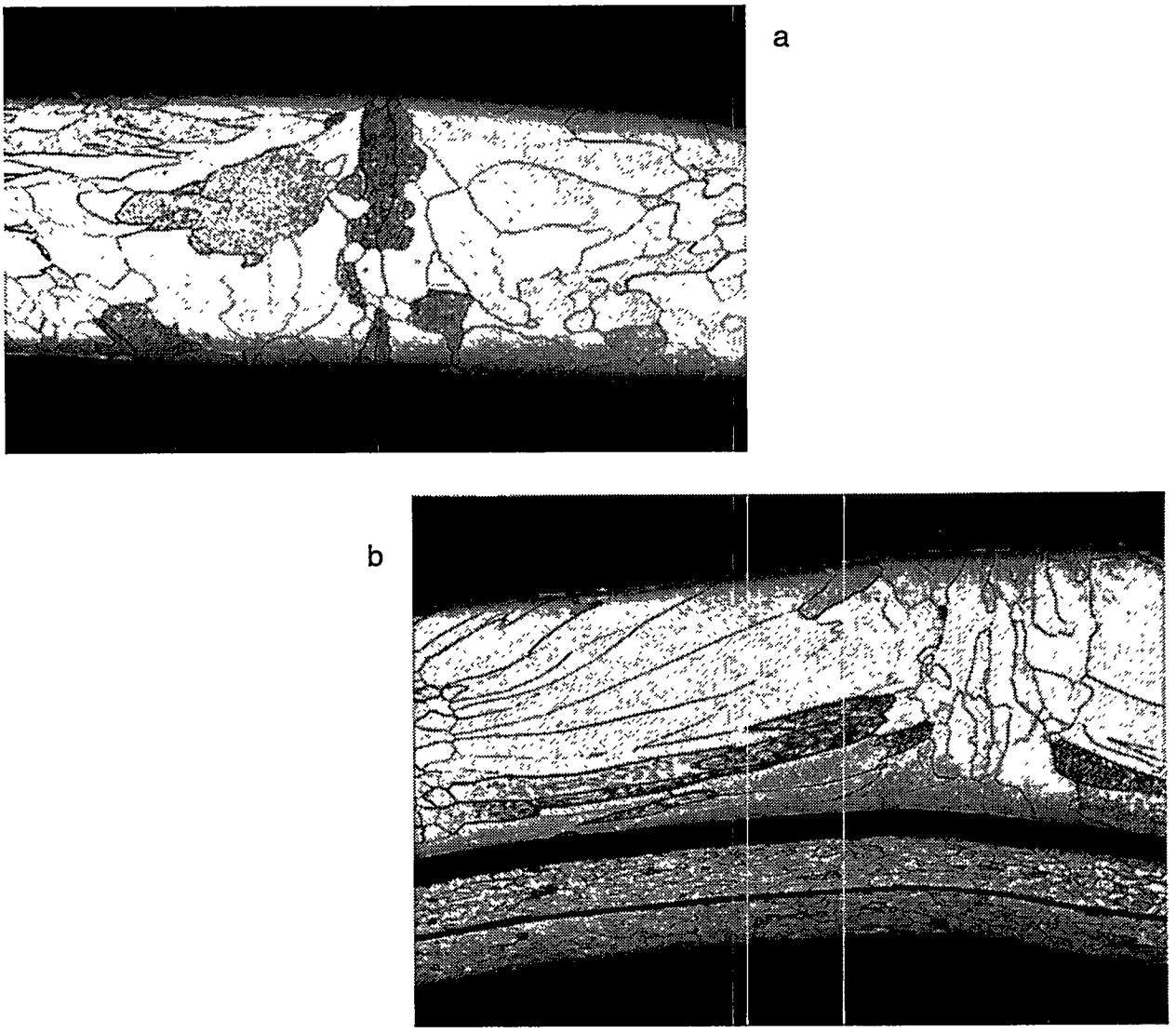

Figure 12. The weld microstructure of capsule SC0076 is typical; etched, 50× magnification. (a) single-pass weld area, (b) weld overlap area. (NMT-9 Negs 9511-81, 9511-77)

Table V. Vent and Shield Cup Microstructure, SC0076		
Area/Orientation	**Grain Size, grains/wall thickness[a]**	**Grain Size, μm/grain**
Shield Cup/Axial	25.0	26.1
Shield Cup/Transverse	25.5	25.6
Vent Cup/Axial	28.5	22.8
Vent Cup/Transverse	28.9	22.6

[a]Grains/nominal wall thickness of 0.65 mm.

TABLE VI. Particle Size Analysis of Urania Recovered from RTG-1 and RTG-2

Particle Size Range (μm)	SC0076 (RTG-1) Retained Fuel[a]	SC0092 (RTG-2) Retained Fuel[b]	SC0096 (RTG-2) Retained Fuel[c]	SC0107 (RTG-2) Retained Fuel[d]
+5600	0.4929	0.5953	0.5296	0.8111
+2000 to 5600	0.3074	0.2623	0.3215	0.1435
+850 to 2000	0.1256	0.0852	0.1033	0.0318
+425 to 850	0.0408	0.0273	0.0257	0.0077
+180 to 425	0.0196	0.0133	0.0122	0.0033
+125 to 180	0.0036	0.0027	0.0027	0.0004
+75 to 125	0.0037	0.0025	0.0016	0.0004
+45 to 75	0.0023	0.0027	0.0012	0.0008
+30 to 45	0.0007	0.0012	0.0006	0.0002
+20 to 30	0.0010	0.0020	0.0004	0.0002
+10 to 20	0.0016	0.0035	0.0005	0.0003
+9 to 10	0.0001	0.0002	0.0000	0.0000
+8 to 9	0.0001	0.0002	0.0000	0.0000
+7 to 8	0.0001	0.0002	0.0000	0.0000
+6 to 7	0.0001	0.0002	0.0000	0.0000
+5 to 6	0.0001	0.0002	0.0001	0.0000
+4 to 5	0.0001	0.0003	0.0001	0.0001
+3 to 4	0.0002	0.0005	0.0003	0.0002
+2 to 3	0.0000	0.0001	0.0001	0.0000
+1 to 2	0.0000	0.0001	0.0001	0.0000
<1	0.0000	0.0000	0.0000	0.0000
Total:	1.0000	1.0000	1.0000	1.0000
Weight fraction <10 μm:	0.0008	0.0020	0.0007	0.0003

[a]No fuel released.
[b]Approximately 12.164g fuel released.
[c]Approximately 0.229g fuel released.
[d]Approximately 0.026g fuel released.

B. Second End-on Impact Test; RTG-2

One half of a Cassini RTG with a simulant heat source stack made up of FWPF graphite modules loaded with urania-fueled clads and molybdenum slugs was impacted against a 3 ft × 4 ft × 18 in. concrete slab on May 24, 1995. The impact velocity was 77.1 m/s and the RTG graphite module stack temperature was 1090 ± 5°C. Capsule deformations are listed in Table VII. The furnace test stand is shown in Figure 13 and the converter mounted on the sled is shown in Figure 14.

TABLE VII. RTG-2 Capsule Strains

			STRAIN, %[a]			
			Vent Cup, Diametral		Shield Cup, Diametral	
Module	GPHS	Axial	Max.	Min.	Max.	Min.
1	SC0090	4.10	7.28	-7.03	6.77	-3.34
1	SC0089	10.65	12.51	-14.48	10.11	-8.83
1	SC0092	14.98	NM[b]	NM[b]	10.03	-4.28
1	SC0091	5.87	10.45	-12.00	5.48	-5.31
2	SC0094	2.47	4.71	-5.91	2.57	-2.31
2	SC0093	1.95	3.43	-2.48	2.48	-2.31
2	SC0096	21.48	10.37	-17.40	9.43	-11.48
2	SC0095	5.18	7.71	-11.31	6.68	-7.03
3	SC0103	2.04	2.83	-4.63	2.48	-1.37
3	SC0097	2.47	3.94	-4.20	4.03	-2.31
3	SC0105	3.90	3.00	-7.63	3.26	-5.06
3	SC0104	4.24	4.28	-6.43	4.54	-7.71
4	SC0108	1.78	0.94	-1.71	2.06	-3.00
4	SC0106	1.45	1.97	-4.46	1.54	-1.80
4	SC0107	4.16	-3.86	6.34	4.80	-6.51
4	SC0086	1.36	3.17	-4.46	3.08	-2.66
5	SC0069	0.76	1.28	-2.23	1.28	-2.06
5	SC0068	3.54	3.08	-4.54	4.28	-7.46
5	SC0071	3.15	4.46	-7.54	3.94	-5.83
5	SC0070	3.99	4.03	-3.68	2.66	-2.74
6	SC0101	0.85	0.51	-0.60	0.26	-0.17
6	SC0100	0.51	0.09	-1.28	-0.09	-0.69
6	SC0109	0.43	2.14	-3.68	1.03	-2.66
6	SC0102	2.38	1.20	-5.74	1.80	-3.60

[a] Engineering strain values based on pre-impact nominal dimensions (length = 1.181 in. and cup diameter = 1.167 in.)
[b] Not measurable, parts of the cup missing.

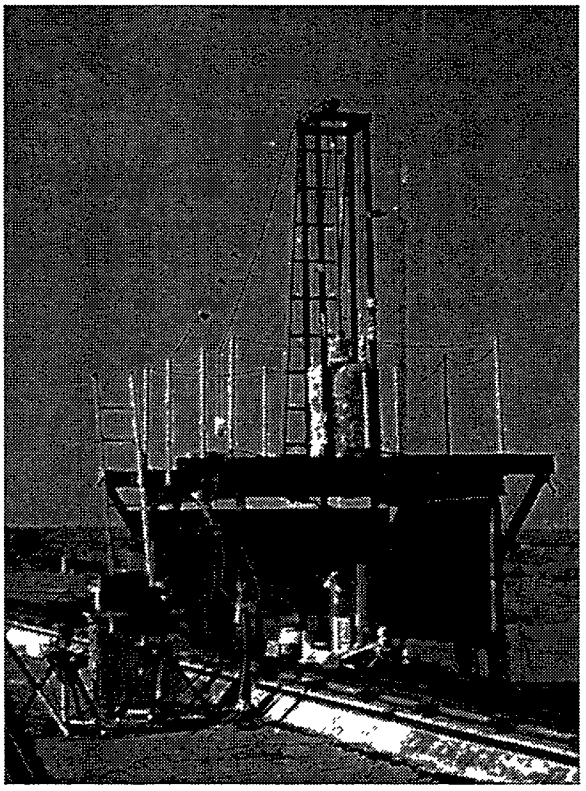

Figure 13. Test stand for Test RTG-2. (NMT-9 Neg B2267, Roll 1, #3)

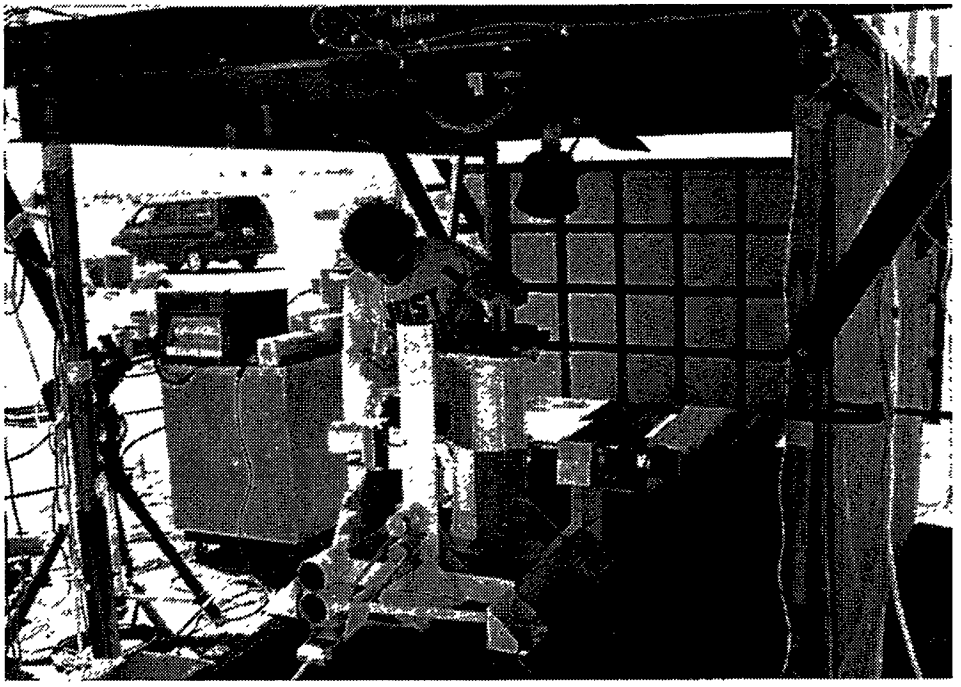

Figure 14. Converter mounted on sled for Test RTG-2. (NMT-9 Neg B2267, Roll 6, #0)

There was considerable failure of the converter housing at the impacted end. The impact resulted in compaction of the housing by approximately six inches. The converter end cap was sheared off and found lying beside the converter (Figure 15). Several of the end cap bolts embedded in the face of the concrete target (Figure 16).

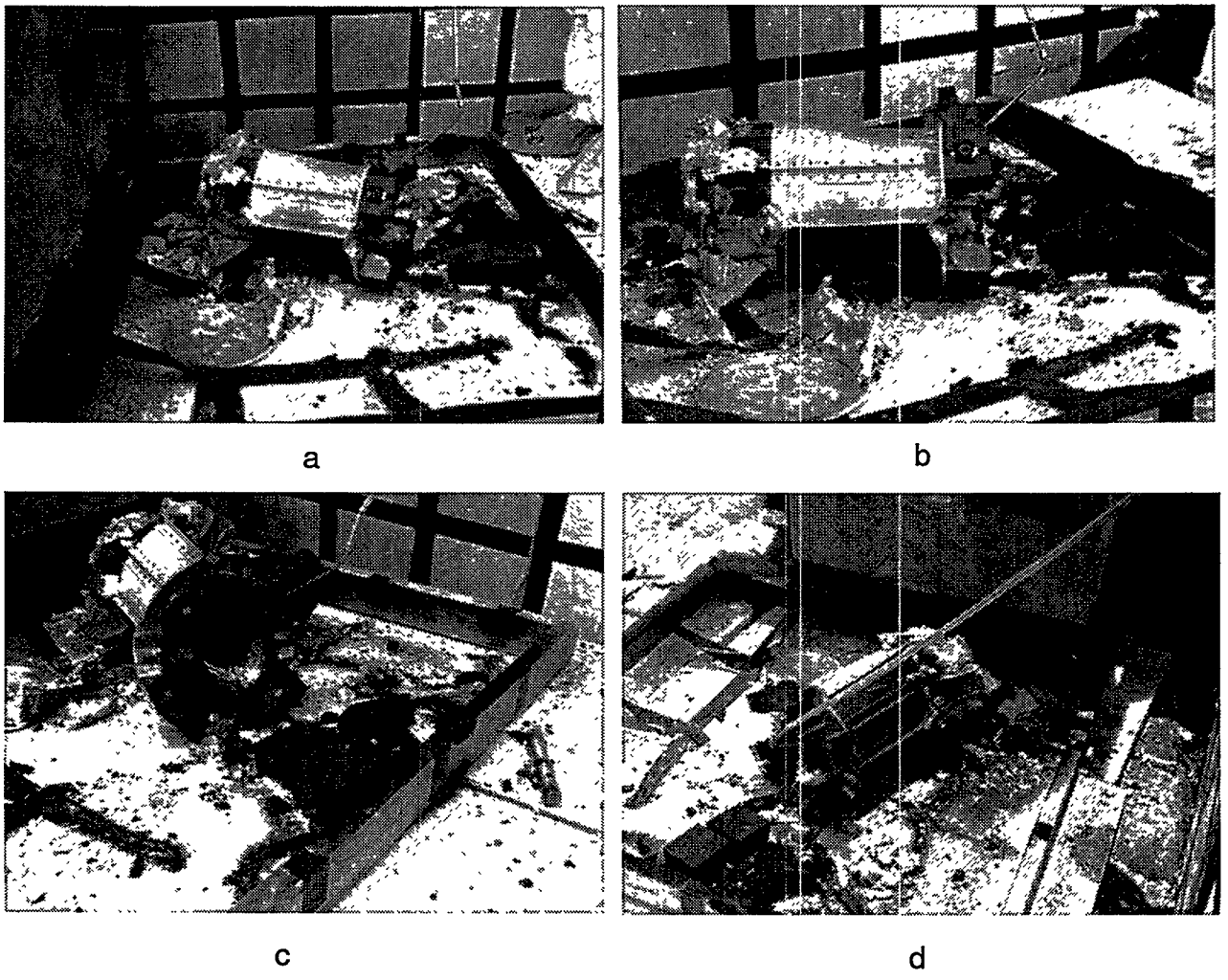

Figure 15. Impacted converter housing, Test RTG-2; (a) side view, (b) close-up of side view, (c) rear view, (d) opposite side view. (NMT-9 Negs B2267, Roll 6, #6; B2267 Roll 4, #6; B2267 Roll 4, #12; B2267 Roll 4, #22)

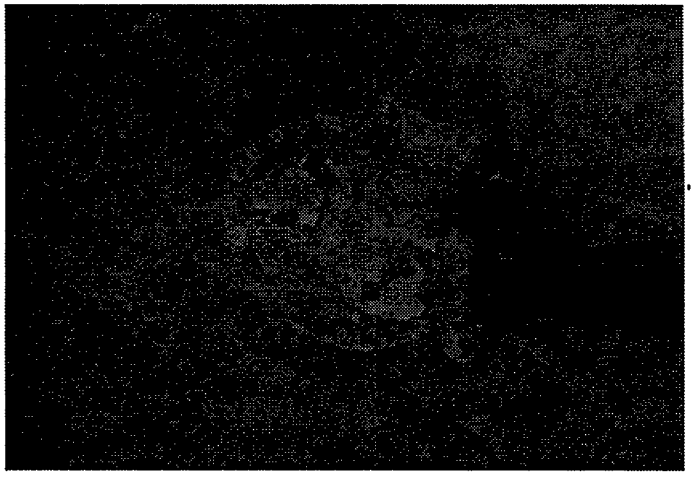

Figure 16. Concrete target, post-impact, Test RTG-2. (NMT-9 Neg B2267, Roll 4, #9)

Four clads were ejected out the front (impacted) end of the converter. Three of these had breaching cracks in the iridium clads (Figure 17). One of the breached clads, SC0092, was missing approximately 1/4 of the vent cup cladding. Another breached clad, SC0096, had a large transverse indentation above the weld on the vent cup. The clad deformation appeared to be caused by the titanium heat source support assembly located in the front end of the converter housing (Figure 18). The remaining breached clad, SC0107, had a weld centerline crack. The fuel was recovered from the three breached clads and submitted for particle size analysis; listed in Table VI.

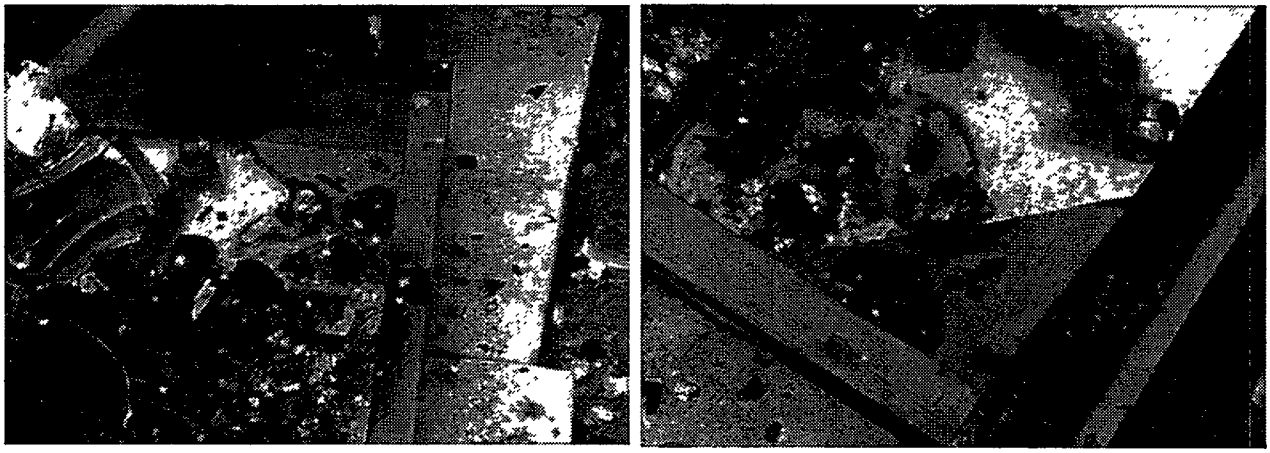

Figure 17. Three clads were ejected from the impacted end of the converter and remained within the wooden barrier in Test RTG-2; (a) SC0107, SC0096, and SC0092 (from left to right), (b) SC0092, SC0096, and SC00107 (from left to right). (NMT-9 Negs B2267 Roll 6, #19; B2267 Roll 4, #2)

a

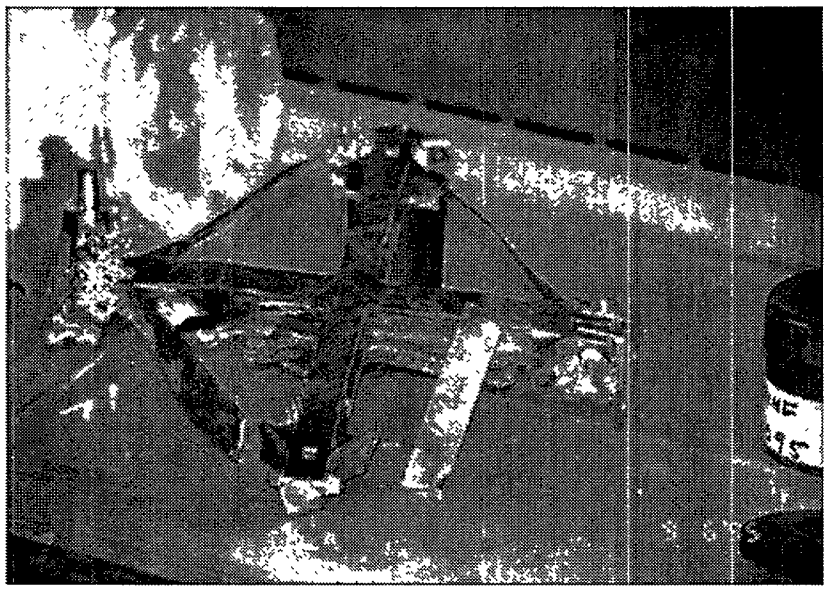

b

Figure 18. Titanium heat source support assembly recovered from test RTG-2; (a) heat source support assembly, post test, (b) heat source support assembly, removed from converter housing. (NMT-9 Negs B2281, Roll 1, #18; B2281, Roll 1, #22)

Four modules were ejected from the back of the converter (Figure 19). One of these was cracked in half and contained one intact GIS. The other GIS was cracked and its clads released. The other three modules were intact. The cracked module was Module 6; the others, Modules 7, 8, and 9, respectively.

SC0092 was located in the open end of the C GIS in Module 1. The impact face of the clad was centered at approximately 0 degrees at the weld start. A large piece of the vent cup was torn off during the impact (Figure 20). The area of this breach was measured to be approximately 485 mm^2. This clad was defueled but not submitted for metallography.

SC0096 was located in the open end of the C GIS in Module 2 (Figure 21). A transverse breaching crack was located in the vent cup in the impact face (0 degrees from weld start). This crack measured approximately 10.81 mm long and had a width of approximately 1.48 mm. The crack appears to have been caused by impact with the relatively sharp edge of an external component upon impact. A titanium heat source support assembly was located in the front end of the converter housing. The widest area of the crack appeared to have been pushed open by fragmentation of the simulant fuel pellet beneath the clad wall.

Five sections were cut from SC0096 and submitted for metallographic examination. Examination of the vent revealed typical microstructure. No anomalies were observed in the vent microstructure.

The microstructure of the breached area revealed intergranular failure. The microstructure along the crack edge shows thinning of the clad wall and grain elongation (Figure 22). The width of the crack in the area examined measured 1.06 mm. The microstructures of the single-pass weld and weld overlap areas were typical of the microstructures usually observed in these areas (Figure 23). The grain size in the single-pass weld area averaged 10.7 grains/wall thickness (80.6 μm/grain), and the grain size in the weld overlap area averaged 9.3 grains/wall thickness (70.0 μm/grain). The microstructures of the vent and shield cup walls were also typical. The average grain sizes of the shield and vent cup walls are given in Table VIII.

Figure 19. Four modules were ejected from the rear end of the converter in Test RTG-2. (NMT-9 Neg B2267, Roll 4, #25)

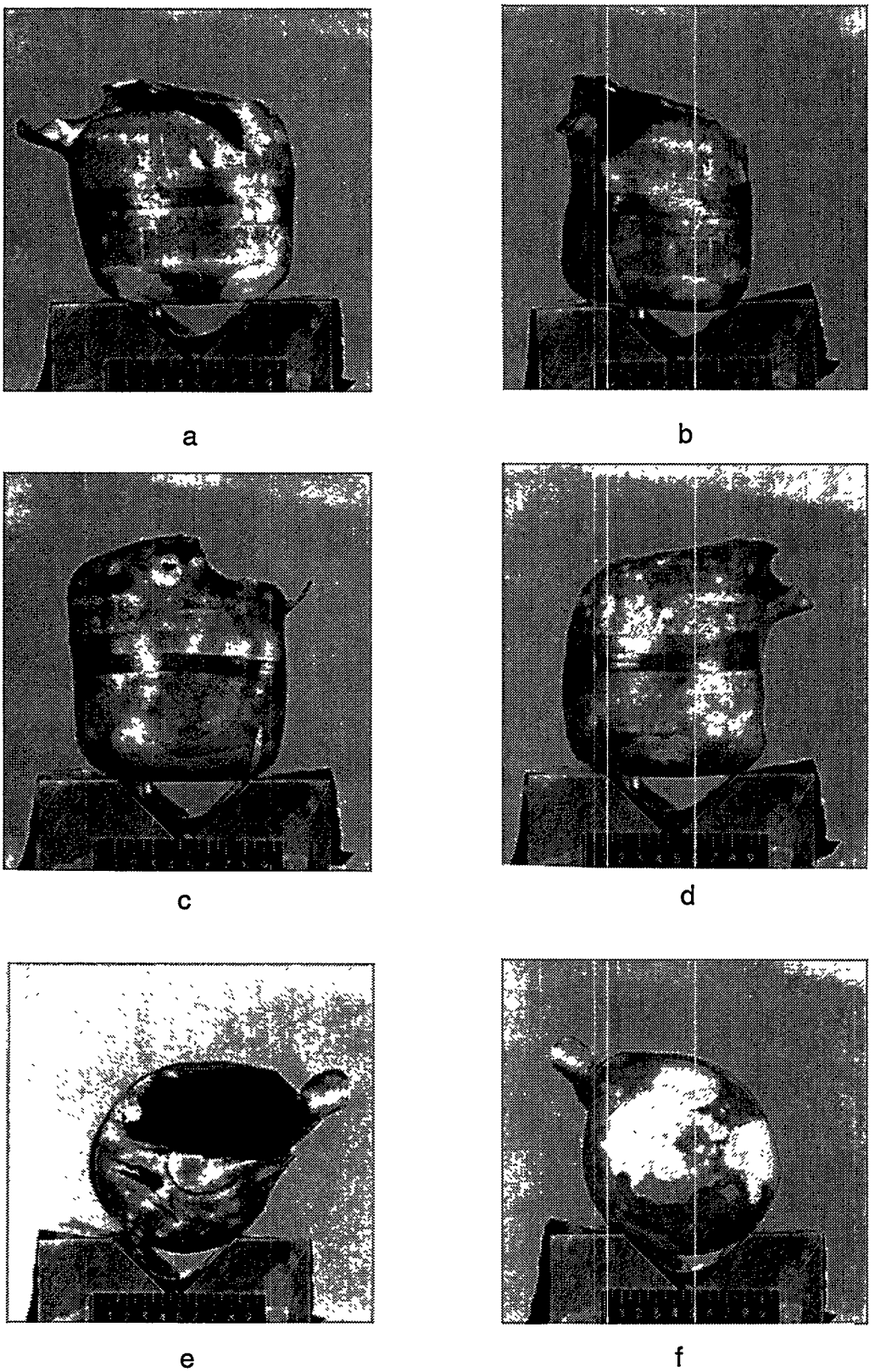

Figure 20. A large piece of the vent cup of SC0092 was sheared off during impact in Test RTG-2; (a) impact face, (b) profile, (c) trailing face, (d) opposite profile, (e) vent end, (f) blind end. (NMT-9 Negs 953-81, 953-82, 953-83, 953-84, 953-79, 953-80)

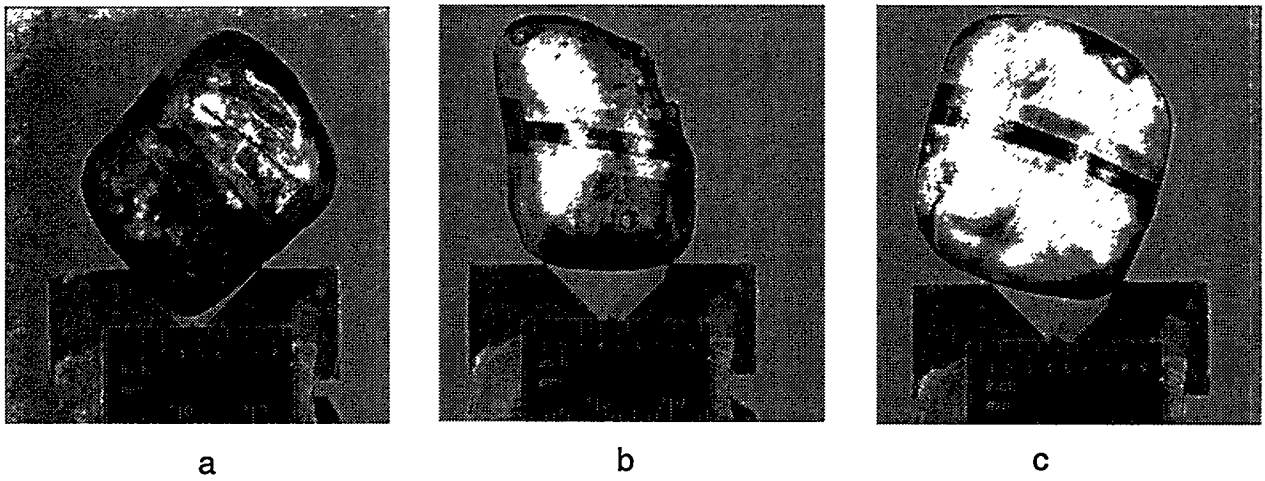

a b c

d e f

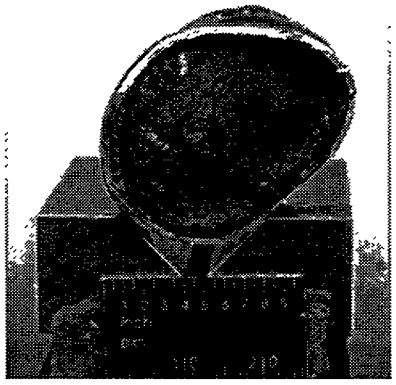

g

Figure 21. A transverse breaching crack was located in the vent cup on the impact face of SC0096; (a) impact face, (b) profile, (c) trailing face, (d) opposite profile, (e) vent end, (f) blind end, (g) fuel fragmentation. (NMT-9 Negs 954-6, 954-9, 954-8, 954-7, 954-5, 954-4, 9510-68)

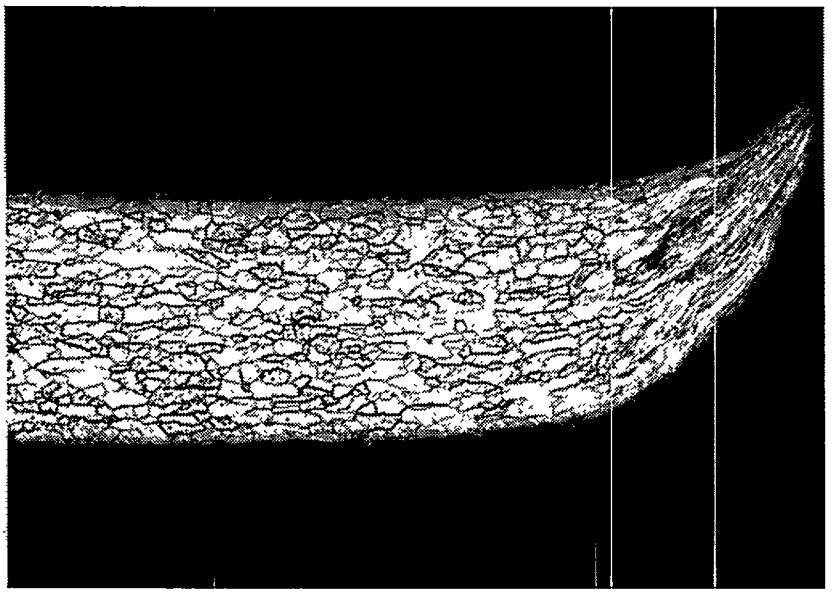

a

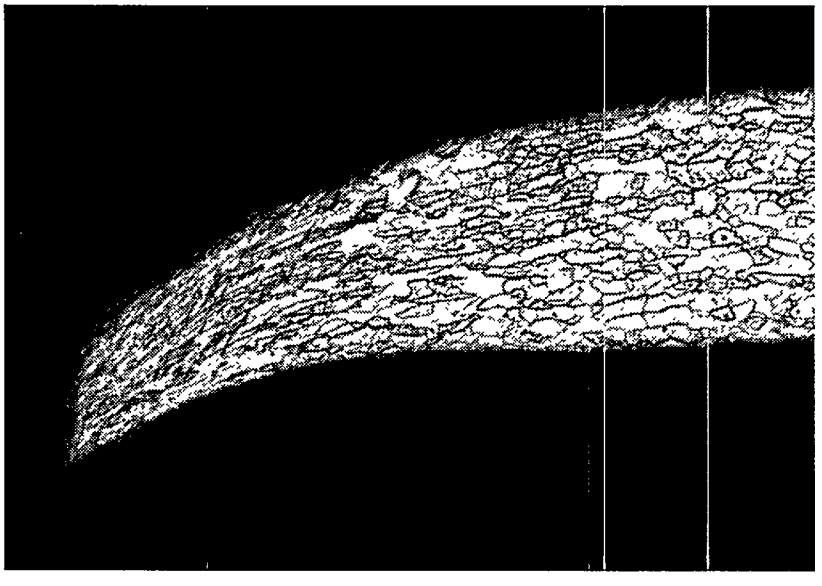

b

Figure 22. Microstructure of breaching crack revealed wall thinning and grain alignment at crack faces; etched, 50× magnification; (a) crack end, (b) opposite end. (NMT-9 Negs 9511-55, 9511-56)

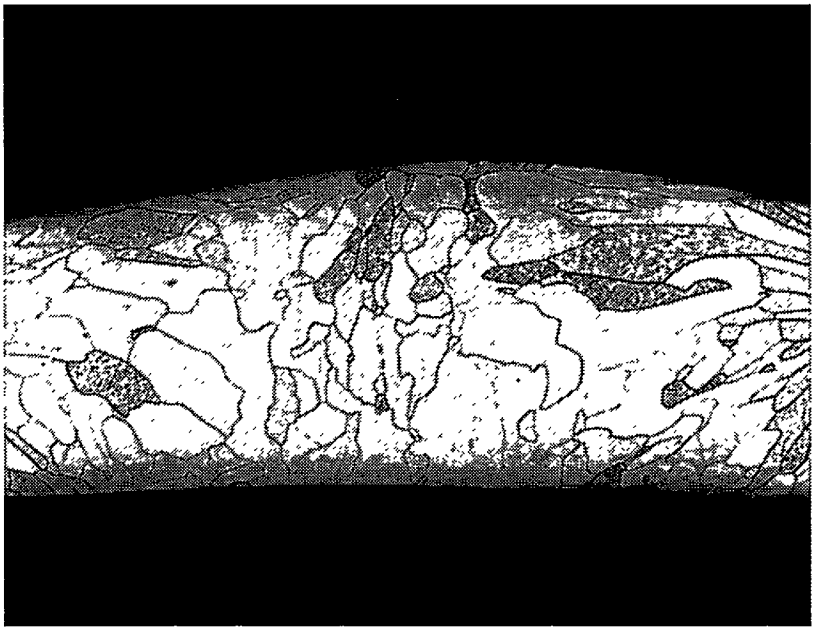

a

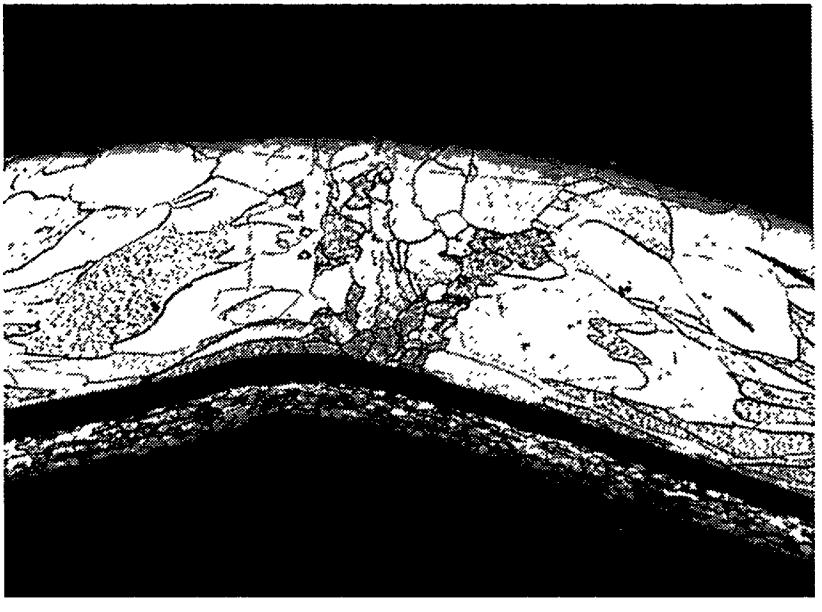

b

Figure 23. Weld microstructure of SC0096; etched, 50× magnification; (a) single pass weld area, (b) weld overlap area. (NMT-9 Negs 9511-57 and 9511-40)

Table VIII. Vent and Shield Cup Microstructure, SC0096 and SC0107		
Area/Orientation	**Grain Size, grains/width[a]**	**Grain Size, μm/grain**
SC0096		
Shield Cup/Axial	27.4	23.7
Vent Cup/Axial	22.7	28.8
SC0107		
Shield Cup/Axial	25.3	25.8
Vent Cup/Axial	27.2	24.0

[a]Grains/nominal wall thickness of 0.65 mm.

SC0107 was one of three simulant-fueled clads that breached. SC0107 was located in the open end of the C GIS in Module 4 (Figure 24). The impact face was centered at approximately 200 degrees from the weld start. A weld centerline crack was centered at approximately 90 degrees from weld start, spanning from approximately 45 to 135 degrees. This crack measured approximately 16.58 mm long and had a width of approximately 1.05 mm. The weld shield was also breached and the urania was visible through the crack. The crack was centered between two flattened areas of the clad and appears to have been caused by compression of the clad.

Four sections were cut from SC0107 and submitted for metallographic examination. Examination of the vent revealed typical microstructure. No anomalies were observed in the vent microstructure.

The microstructure of the breached area revealed a clean intergranular fracture with little, if any, wall thinning and grain elongation. Fusion of the weld shield to the weld was also observed in this location. The microstructure along the crack edge shows cleavage between the grains typical of iridium failure (Figure 25). The width of the crack in the area examined measured 1.26 mm. Another crack was observed underneath the weld shield, outside of the weld, in another area of the clad (Figure 26). This crack initiated in the interior of the clad and had approximately 29% penetration.

The microstructures of the single-pass weld and weld overlap areas were typical of the microstructures usually observed in these areas (Figure 27). The grain size in the single-pass weld area averaged 10.7 grains/wall thickness (71.9 mm/grain), and the grain size in the weld overlap area averaged 9.8 grains/wall thickness (82.0 mm/grain). The microstructures of the vent and shield cup walls was also typical. The average grain sizes of the vent and shield cup walls are given in Table VIII.

V. DISCUSSION

A. Impact Response and Fuel Release

There were no capsule failures in test RTG-1, although four capsules experienced dimensional strains greater than 10%. These capsules were located in Modules 1 and 2 on the impact end of the converter. One capsule in particular, SC0076, had a diametral strain above 20%. This strain would be expected to result in a failure. Previous testing with simulant-fueled capsules, in

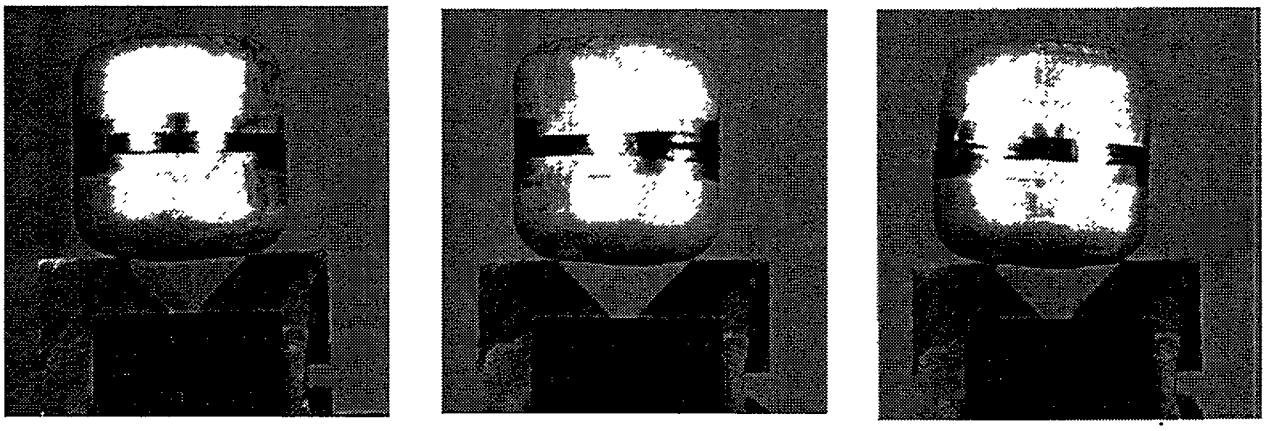

a b c

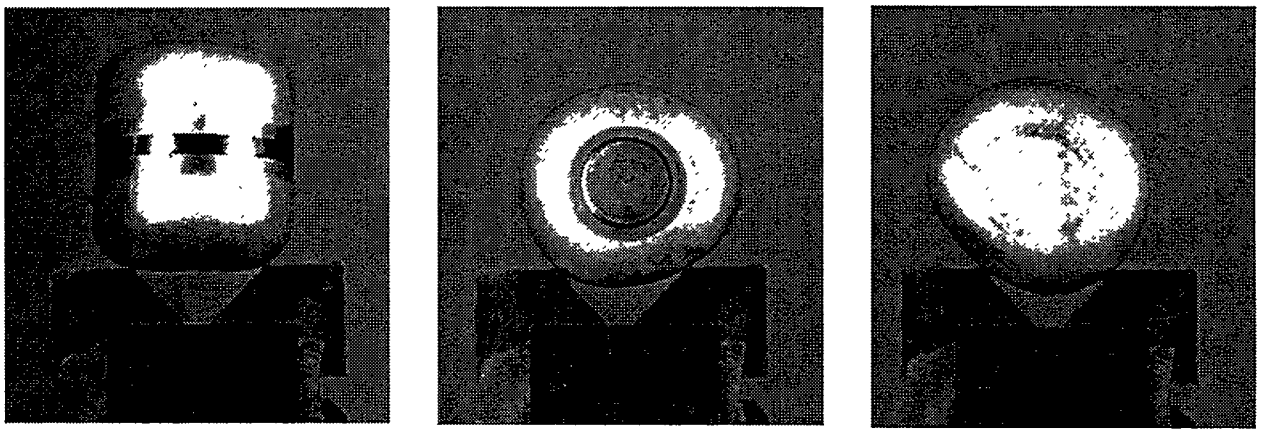

d e f

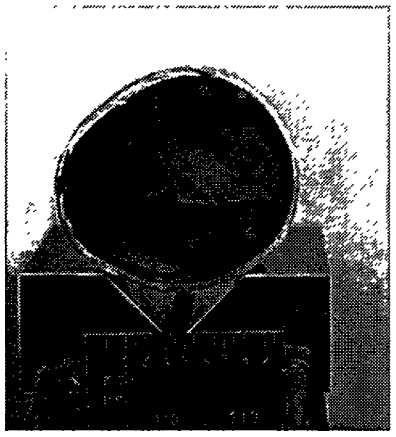

g

Figure 24. A weld centerline crack was centered at approximately 90 degrees from the weld start in SC0107; (a) impact face, (b) profile, (c) trailing face, (d) opposite profile, (e) vent end, (f) blind end, (g) fuel fragmentation. (NMT-9 Negs 954-60,

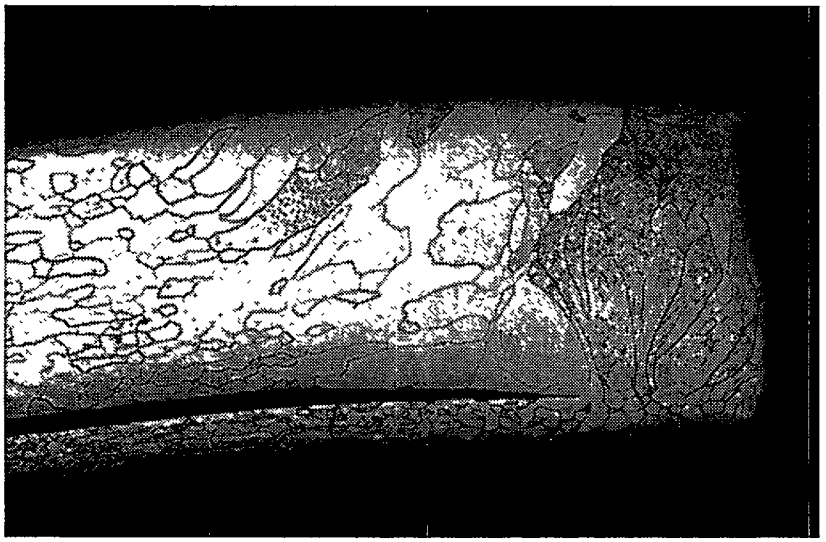

a

b

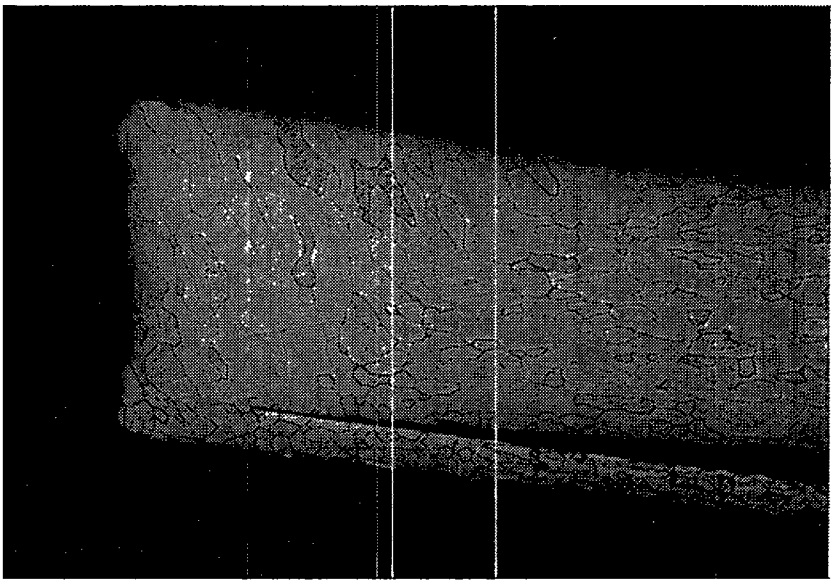

Figure 25. Weld centerline crack ends show intergranular failure; etched, 50× magnification; (a) crack end, (b) opposite end. (NMT-9 Negs 9512-06 and 9512-07)

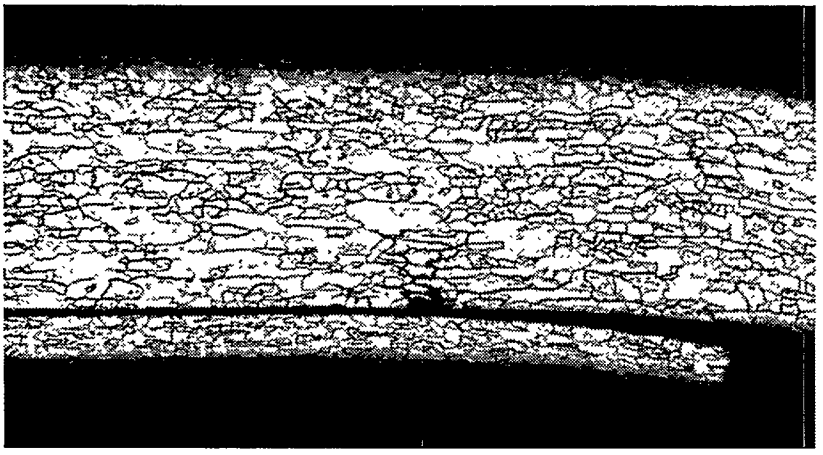

Figure 26. Nonpenetrating crack observed in the shield cup under the weld shield; etched, 50× magnification. (NMT-9 Neg 9512-10)

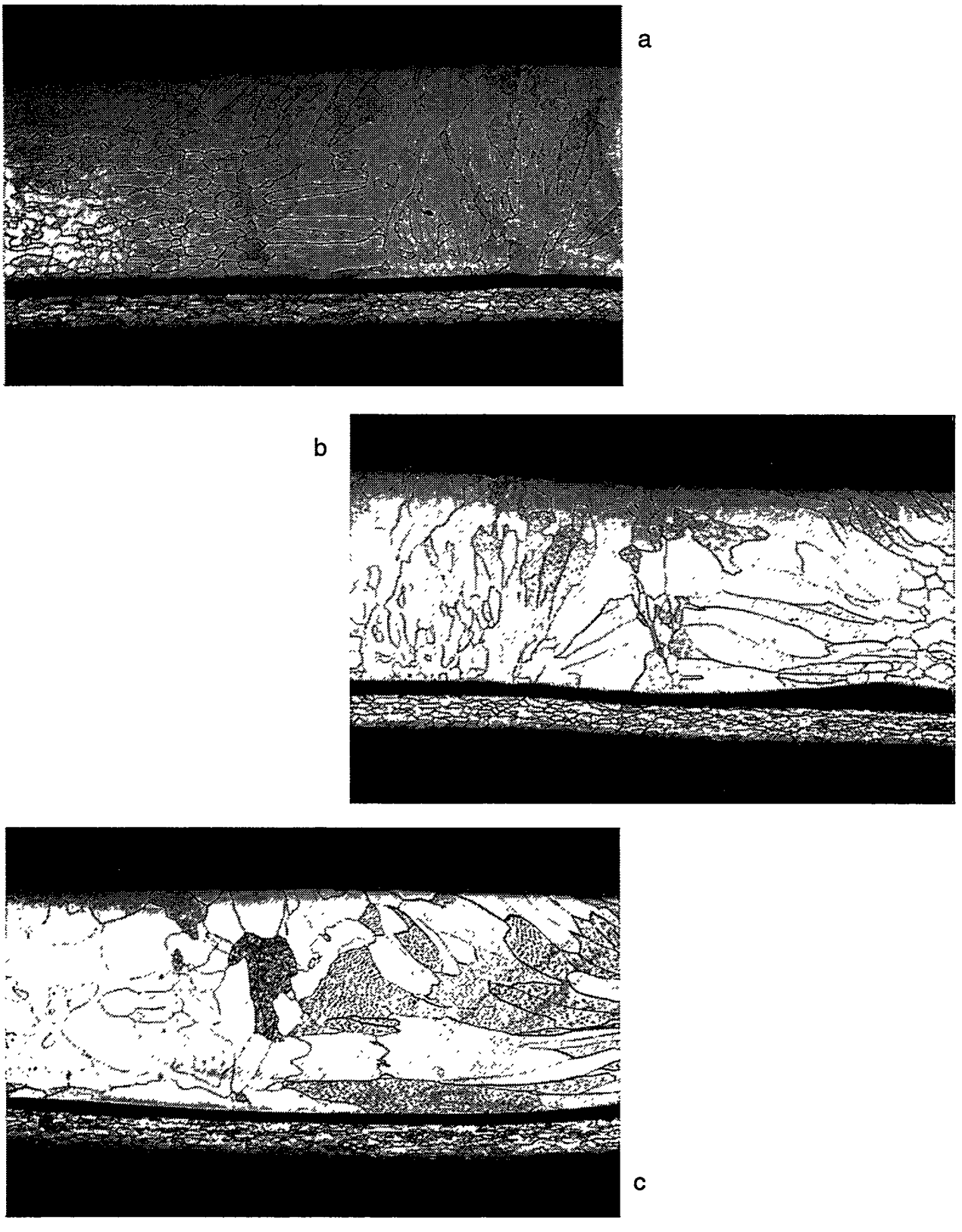

Figure 27. Weld microstructure of SC0107; etched, 50× magnification; (a) single pass weld area, (left side) (b) single pass weld area, (right side) (c) weld overlap area. (NMT-9 Negs 9512-13, 9512-12, and 9512-08)

the cold-process verification (CPV) test series, resulted in failures at strains ranging from 12 to 16%.[15] However, a full module impact in the CPV test series, at 54 m/s, did not result in clad failures.

Three of the capsules in test RTG-2 had capsule failures. Two of the clads, SC0092 and SC0096, appeared to fail due to contact with the titanium heat source support assembly. Capsule SC0092 had a large failure area (485 mm^2) that resulted in a release of approximately 12 g of simulant fuel. Capsule SC0096 had a much smaller failure that resulted in a release of approximately 0.2 g of simulant fuel. Capsule SC0107 experienced a weld failure. The intergranular failure occurred between columnar grains located in the weld centerline. Fusion of the weld with the weld shield was also evident in this location. This failure appeared to be the result of fragment push-through and resulted in a release of approximately 0.026 g.

The releases from SC0092 and SC0096 are higher, from two to 120 times greater than releases observed in previous tests,[15] such as the CPV test series. The breaches of these capsules were also relatively larger than those observed in previous tests. This appears to be caused by the different geometry of the impact "target". The RTG-1 clads appeared to impact against an arm of the titanium heat source support assembly, whereas the CPV clads were impacted against a flat, hardened steel target. The release from SC0107 is smaller than previous releases and the breach area is within the range of those observed in the CPV test series. There was no evidence that this clad impacted on the support assembly.

B. Pellet Fragmentation

Based on data presented in Table VI, there is a slight difference between the particle size profiles of urania recovered from RTG-1 (SC0076) and two of the breached clads recovered from RTG-2 (SC0092 and SC0096). The most significant difference is in the ≤10 mm range size. The fraction of urania recovered from SC0092 is just over twice the amount recovered from SC0076 and SC0096. However, the magnitude of these weight fractions are very small in comparison to the weight fractions measured in the CPV tests (two to 9.2 times smaller).[15]

There is a significant difference between the fragmentation of SC0107, recovered from RTG-2, and the other clads recovered from RTG-1 and RTG-2. The fraction of urania recovered from SC0107 in the +5600 mm range is almost twice that recovered from SC0076, SC0092, and SC0096. Capsule SC0107 did not undergo the same magnitude of deformation as the others. Because the clad was not deformed as severely as the other clads, the fuel pellet would not be expected to be as fragmented as the other fuel pellets.

Table IX compares the particle size distribution of the urania recovered from tests RTG-1 and RTG-2 to the distribution of urania recovered from a clad impacted in a full module impact (SC0074). The particle size distribution of SC0074 is very similar to the other distributions and there is no apparent difference between them.

TABLE IX. Pellet Fragmentation of Simulant-Fueled Clads in Modules

Particle Size Range, μm	WEIGHT FRACTION Retained Fuel RTG-1 SC0076	RTG-2 SC0092	RTG-2 SC0096	RTG-2 SC0107	CPV SC0074[a]
+180	0.9863	0.9834	0.9923	0.9974	0.9946
+125 to 180	0.0036	0.0027	0.0027	0.0004	0.0018
+75 to 125	0.0037	0.0025	0.0016	0.0004	0.0015
+45 to 75	0.0023	0.0027	0.0012	0.0008	0.0011
+30 to 45	0.0007	0.0012	0.0006	0.0002	0.0001
+20 to 30	0.0010	0.0020	0.0004	0.0002	0.0002
+10 to 20	0.0016	0.0035	0.0005	0.0003	0.0003
≤10	0.0008	0.0020	0.0007	0.0003	0.0004
TOTAL	1.0000	1.0000	1.0000	1.0000	1.0000

[a]Clad recovered from a full module impact against a steel target, 54 m/s. Refer to reference 15.

VI. CONCLUSIONS

1. Impact of one half of a converter housing loaded with simulant GPHSs at 57.6 m/s resulted in no GPHS clad failures.
2. Impact of the converter housing loaded with simulant GPHSs at 77.1 m/s resulted in the failure of three GPHSs. Two of the failures appear to have been caused by impact with the titanium heat source support assembly.
3. The results suggest that the RTG and graphite components surrounding the GPHS protect against clad failure at velocities up to 57 m/s. This protection appears to be overcome at higher impact velocities, allowing GPHS clads to impact with converter housing components that have unfavorable strength/hardness and geometry, thereby resulting in clad failures.

VII. ACKNOWLEDGMENTS

We thank A. Herrera, M. Barney, and D. Montoya for designing and conducting the field tests, and T. Baros, E. Burciaga, C. Lynch, P. Moniz, and M. Padilla for performing metallography, sample preparation, and particle size analyses. We would like to give special thanks to B. Kampfe and F. Mathews of Sandia National Laboratory for design of the sleds and coordination of tests at the Sandia sled test facility.

REFERENCES

1. C. T. Bradshaw, "Safety Test Program Plan for the Cassini RTG Program," Martin Marietta Astro Space report CDRL No. A. 10, GESP-7223 (May 1993).

2. F. W. Schonfeld, "General-Purpose Heat Source Development: Safety Test Program, Postimpact Evaluation, Design Iteration Test 1," Los Alamos National Laboratory report LA-9680-SR (April 1984).

3. F. W. Schonfeld and T. G. George, "General-Purpose Heat Source Development: Safety Test Program, Postimpact Evaluation, Design Iteration Test 2," Los Alamos National Laboratory report LA-10012-SR (June 1984).

4 F. W. Schonfeld and T. G. George, "General-Purpose Heat Source Development: Safety Test Program, Postimpact Evaluation, Design Iteration Test 3," Los Alamos National Laboratory report LA-10034-SR (July 1984).

5. T. G. George and F. W. Schonfeld, "General-Purpose Heat Source Development: Safety Test Program, Postimpact Evaluation, Design Iteration Test 4," Los Alamos National Laboratory report LA-10217-SR (December 1984).

6. T. G. George and F. W. Schonfeld, "General-Purpose Heat Source Development: Safety Test Program, Postimpact Evaluation, Design Iteration Test 5," Los Alamos National Laboratory report LA-10232-SR (December 1984).

7. D. Pavone, T. G. George, and C. E. Frantz, "General-Purpose Heat Source Safety Verification Test Series: SVT-1 Through SVT-6," Los Alamos National Laboratory report LA-10353-MS (June 1985).

8. T. G. George and D. Pavone, "General-Purpose Heat Source Safety Verification Test Series: SVT-7 Through SVT-10," Los Alamos National Laboratory report LA-10408-MS (September 1985).

9. T. G. George and D. Pavone, "General-Purpose Heat Source Safety Verification Test Series: SVT-11 Through SVT-13," Los Alamos National Laboratory report LA-10710-MS (May 1986).

10. T. G. George, R. E. Tate, K. M. Axler, "General-Purpose Heat Source Development: Safety Verification Test Program; Bullet/Fragment Test Series," Los Alamos National Laboratory report LA-10364-MS (May 1985).

11. T. G. George, "General-Purpose Heat Source Development: Safety Verification Test Program; Titanium Bullet/Fragment Test Series," Los Alamos National Laboratory report LA-10724-MS (June 1986).

12. T. A. Cull, T. G. George, and D. Pavone, "General-Purpose Heat Source Development: Safety Verification Test Program; Explosion Overpressure Test Series," Los Alamos National Laboratory report LA-10697-MS (September 1986).

13. T. A. Cull and D. Pavone, "General-Purpose Heat Source Development: Safety Verification Test Program; Flyer Plate Test Series," Los Alamos National Laboratory report LA-10742-MS (September 1986).

14. T. G. George, "General-Purpose Heat Source Development: Safety Verification Test Program; Edge-On Flyer Plate Tests," Los Alamos National Laboratory report LA-10872-MS (March 1987).

15. M. A. H. Reimus and T. G. George, "General-Purpose Heat Source: Research and Development Program; Cold-Process Verification Test Series," Los Alamos National Laboratory report LA-13118-MS (In press).